

Disentangling Oil Weathering at a Marine Seep Using GC \times GC: Broad Metabolic Specificity Accompanies Subsurface Petroleum Biodegradation

GEORGE D. WARDLAW,[†]

J. SAMUEL AREY,[‡]

CHRISTOPHER M. REDDY,[§]

ROBERT K. NELSON,[§]

G. TODD VENTURA,[§] AND

DAVID L. VALENTINE*,[†]

Department of Earth Science and the Marine Science Institute, University of California, Santa Barbara, California 93106, Environmental Chemistry Modeling Laboratory, GR C2 514, Swiss Federal Institute of Technology, Lausanne, Switzerland, and Department of Marine Chemistry and Geochemistry, Woods Hole Oceanographic Institution, MS#4, Woods Hole, Massachusetts 02543

Received May 20, 2008. Revised manuscript received July 30, 2008. Accepted July 31, 2008.

Natural seeps contribute nearly half of the oil entering the coastal ocean. However, environmental fate studies generally monitor fewer than 5% of these petroleum compounds. Hence, the rates and relevance of physical, chemical, and biological weathering processes are unknown for the large majority of hydrocarbons, both released from natural seeps and also from human activities. To investigate the specific compositional changes occurring in petroleum during subsurface degradation and submarine seepage, we studied the natural oil seeps offshore Santa Barbara, California with comprehensive, two-dimensional gas chromatography (GC \times GC). With this technique, we quantified changes in the molecular diversity and abundance of hydrocarbons between subsurface reservoirs, a proximal sea floor seep, and the sea surface overlying the seep. We also developed methods to apportion hydrocarbon mass losses due to biodegradation, dissolution, and evaporation, for hundreds of tracked compounds that ascended from the subsurface to the sea floor to the sea surface. The results provide the first quantitative evidence of broad metabolic specificity for anaerobic hydrocarbon degradation in the subsurface and reveal new trends of rapid hydrocarbon evaporation at the sea surface. This study establishes GC \times GC as a powerful technique for differentiating biological and physical weathering processes of complex mixtures at a molecular level.

Introduction

Petroleum is produced by the thermal decay of buried organic material and is a mobile complex mixture composed of numerous hydrocarbons having diverse molecular structures

(1). In subsurface and surface environments, the composition of petroleum can be altered by chemical, physical, and biological processes such as oxidation, photolysis, evaporation, dissolution, and biodegradation that are collectively termed weathering (1). Distinguishing the role of each process is important for understanding the biogeochemical cycling of petroleum in nature, whether it is from a geologic, economic, or environmental perspective. For example, information on such processes is essential when determining whether to restore, rehabilitate, or renew oil-impacted areas, as required under legislation enacted in many countries, such as the United States Oil Pollution Act of 1990 (33 USC 2701–2761).

Weathering is most commonly diagnosed by comparing the relative abundance of carefully chosen compound sets between differently weathered oils. The resulting ratios have led to significant advances in the study of oil weathering (2). Compound ratios conventionally employ the molecules that can be resolved by traditional one-dimensional gas chromatography with either flame ionization (GC-FID) or mass spectral (GC-MS) detection. However, these conventional methods do not fully resolve the complex molecular mixture comprising weathered petroleum residues. Consequently, studies usually focus on only a small fraction of the relevant compounds (3, 4).

Recent work indicates that comprehensive, two-dimensional gas chromatography (GC \times GC) effectively overcomes these limitations (5). GC \times GC increases the number of resolvable and accurately quantifiable petroleum hydrocarbons by greater than an order of magnitude (6–8). This capability is particularly beneficial when analyzing biodegraded petroleum, which includes thousands of compounds but often lacks many of the readily quantified, and easily degraded, components such as *n*-alkanes (8). In addition, GC \times GC chromatograms can be used to estimate phase partitioning properties of the analyzed petroleum hydrocarbons. Arey et al. (9) showed that GC \times GC two-dimensional retention indices provide robust estimates on the liquid vapor pressures, aqueous solubilities, octanol–water partition coefficients, and vaporization enthalpies for a wide range of petroleum hydrocarbons, which in turn, allow for detailed studies of phase transfer processes affecting petroleum hydrocarbon mixtures in the environment. This technique was recently used to disentangle the compositional signatures of oil evaporation and dissolution following a marine oil spill (5, 9, 10).

In addition to the limitation of traditional analytical techniques, the ability to adequately schedule field investigations of petroleum weathering processes is often difficult. Field sampling typically does not occur for many hours or days after an oil spill and valuable information on initial processes such as evaporation and dissolution can be lost during a delay. To properly diagnose these time-sensitive weathering processes, we have focused our efforts on the massive oil seeps off the coast of Santa Barbara, CA (see Supporting Information (SI) Figure SI-S1). Marine oil seeps are naturally occurring, steady state chemostats and therefore offer advantageous laboratories for oil weathering studies (11). Here, we compare the molecular composition of petroleum samples that have undergone biological and physical weathering during their stepwise ascent from a subsurface reservoir to the sea floor and then to the sea surface. We differentiate biological and physical petroleum weathering effects in the subsurface, and thereby detail the metabolic preferences of petroleum consuming anaerobes. We then identify the compositional modification to the oil

* Corresponding author phone: (805)893-2973; fax: (805)893-2314; e-mail:valentine@geol.ucsb.edu.

[†] University of California.

[‡] Swiss Federal Institute of Technology.

[§] Woods Hole Oceanographic Institution.

as it rises to the sea surface and is exposed to the atmosphere. Such compositional changes have been only quantified in the field for a few compounds and the terms of their specific weathering processes have not yet been differentiated.

Experimental Section

Study Site. The Coal Oil Point (COP) seep field (see SI Figure SI-S1A–C) is an approximately 18 km² area off the shore of Goleta, CA and ranges in depth from 5 to 80 m (11, 12). The seep field emits 50–170 barrels of oil and 100–130 tons of natural gas per day (11). The geologic structure of the seep field includes a series of crested anticlines formed during folding of the Miocene-age Monterey Formation overlain with recent deposits (11). The Monterey Formation serves as both source rock and geologic trap for local petroleum deposits (11, 13). Oil-bearing reservoirs embedded within anticlines are located at depths between 1.0 and 1.7 km where the ambient temperature ranges between 60 and 75 °C (14). Oil and gas migrate upward through fractures in the diatomaceous chert of the Monterey Formation (11, 13). Geologic evidence indicates that hydrocarbon seepage has occurred in this region for at least the past several hundred thousand years (15, 16), and molecular biological evidence suggests that microorganisms are presently active in the reservoir (14, 17).

Sample Collection. Field samples were collected from subsurface oil reservoirs at COP, at a nearby active sea floor oil seep, and at the sea surface overlying the seep. Oil reservoir samples were collected from three active oil wells accessed by Platform Holly (34°22' N, 119°52' W). The wells 3242-9, 3242-15, and 3242-18 draw petroleum from depths of 1.0–1.1, 1.2–1.3, and 1.0–1.2 km, respectively, and have an ambient temperature of 60–70 °C. Four field samples were collected at a location informally known as Jackpot Seep (34°24.175' N, 119°52.670' W; see SI Figure SI-S1A–C); oil emitted from this seep was hypothesized to originate from the same source rock feeding the wells of Platform Holly. Scuba divers collected two Jackpot Seep oil samples as they oozed up through an area of exposed bedrock at 15 m depth (see SI Figure SI-S1B). Two additional samples were grabbed from the sea surface above Jackpot Seep, within seconds of their ascent (see SI Figure SI-S1C). Care was taken to collect only the freshly exposed sample, but an existing surface slick was present and some exchange may have occurred. To assess the genetic similarities of these seven samples, we compared them to a less-degraded reservoir oil from outside the seep area (Platform Gail; E-16 L, 34°07.500' N, 120°24.020' W, 66 °C; 1.7 km sub seafloor) and to a sample of Arabian light crude.

Comprehensive, Two-Dimensional Gas Chromatography (GC \times GC). The petroleum hydrocarbons were separated with GC \times GC (8), a chromatographic technique that separates compounds based on two distinct properties: boiling point and polarity in this instance. This technique is well suited for resolving complex mixtures such as petroleum, as detailed by Nelson et al. (8) and Gaines et al. (18). The GC \times GC system (8) employed an Agilent 6890 gas chromatograph configured with a 7683 series split/splitless autoinjector, two capillary gas chromatography columns, a model KT-CLM-ZOE02 loop jet modulator (Zoex Corporation, Lincoln, NE), and a flame ionization detector (FID). Each sample was diluted in hexane and spiked with an internal standard, dodecadihydrotriphenylene (DDTP). Each sample was then injected in splitless mode and the purge vent was opened at 2.5 min. The inlet temperature was 300 °C. The first-dimension column and the loop jet modulator reside in the main oven of the Agilent 6890 gas chromatograph. The second-dimension column is housed in a smaller oven installed within the main oven. With this configuration, the temperature profiles of the first-dimension column, thermal modulator (hot jet), and the

second-dimension column were independently programmed. The first-dimension column was a nonpolar 100% dimethyl polysiloxane phase (Restek Rtx-1 Crossbond, 6.5 m length, 0.10 mm i.d., 0.4 μm film thickness) that was programmed to remain isothermal at 37 °C for 5 min and then ramped from 37 to 307 at 1.5 °C min⁻¹. The modulation loop was deactivated fused silica (1.6 m length, 0.10 mm i.d.). The thermal modulator (hot jet) was heated to 100 °C above the temperature in the main oven to ensure that all trapped compounds were thoroughly and rapidly desorbed from the cold spot. Second-dimension separations were performed on a 50% phenyl polysilphenylene-siloxane column (SGE BPX50, 0.8 m length, 0.10 mm I.D., 0.1 μm film thickness) that was programmed to remain isothermal at 70 °C for 5 min and then ramped from 70 to 340 at 1.5 °C min⁻¹. The thermal modulator loop pulse frequency was 10 s (0.10 Hz), and the pulse width was 300 ms. The cold jet gas was dry N₂ chilled with liquid argon at a flow rate of 4.0 L min⁻¹. The carrier gas was H₂ at a constant flow rate of 1.5 mL min⁻¹. The FID signal was sampled at 100 Hz. Peaks were identified with approximately 200 commercially available standards from Aldrich Chemical (*n*-alkanes, hopanes, steranes, and a large suite of PAHs), National Institute of Standards and Technology (ether lipid derivatives, linear alkylbenzenes), and Chiron (alkylcyclohexanes and alkylcyclopentanes) and synthesized standards provided by Professor Roger Summons (Massachusetts Institute of Technology; other alkylcyclopentanes). For reference, the internal standard DDTP eluted at 92.4 min on the *x*-axis and at 5.7 s on the *y*-axis (Figures 1 and 2). We assumed that the response factor for every compound was that of the DDTP, which should be within 20% for such compounds on a FID, based on laboratory studies of pure standards. We define all of the peak volumes that can be integrated in the GC \times GC images to represent the total petroleum hydrocarbons (TPHs) minus the solvent peak and standard.

Results and Discussion

In this study, we followed the fate of petroleum as it traveled from a subsurface oil reservoir to the ocean floor seep and then rose to the sea surface. Our goal was to track the changes in the oil composition, and explain the corresponding weathering processes, for the oil that underwent these transport processes.

Oil Samples Share a Common Source. We hypothesized a common source for our oil samples because of the close proximity of the sites, and because of geological evidence indicating connectivity of the reservoir to the sea floor (19). To confirm that the samples we collected at Platform Holly, the seafloor seep, and sea surface were similar, the diversity and abundance of several specific molecular compound classes and the carbon isotope ratios of bulk petroleum ($\delta^{13}\text{C}$; -23.4 to -22.7‰ VPDB) were analyzed. All of the parameters indicate that the petroleum was generated from the Monterey Formation (see SI Figures SI-S2–S7), and all samples were determined to be highly similar based on statistical comparisons of biomarker distributions (see SI Figures SI-S3–S8).

Oil Sample Selection and Comparison. In order to compare individual compound concentrations between a set of samples, the chromatographic conditions/retention times must be exactly the same for all runs. The reservoir petroleum sample 3242-15 was thus chosen as a reference sample for comparing the chemical differences to the sea floor and sea surface samples, because the two-dimensional retention times of known compounds in this chromatogram matched most closely with those in the Jackpot Seep samples. Chromatographic analysis of sample 3242-15 (Figure 1A) resolved over six thousand peaks, of which \approx 4500 met the criteria to be considered as distinct compounds (see SI section SI-2). Errors in peak resolution derive primarily from the

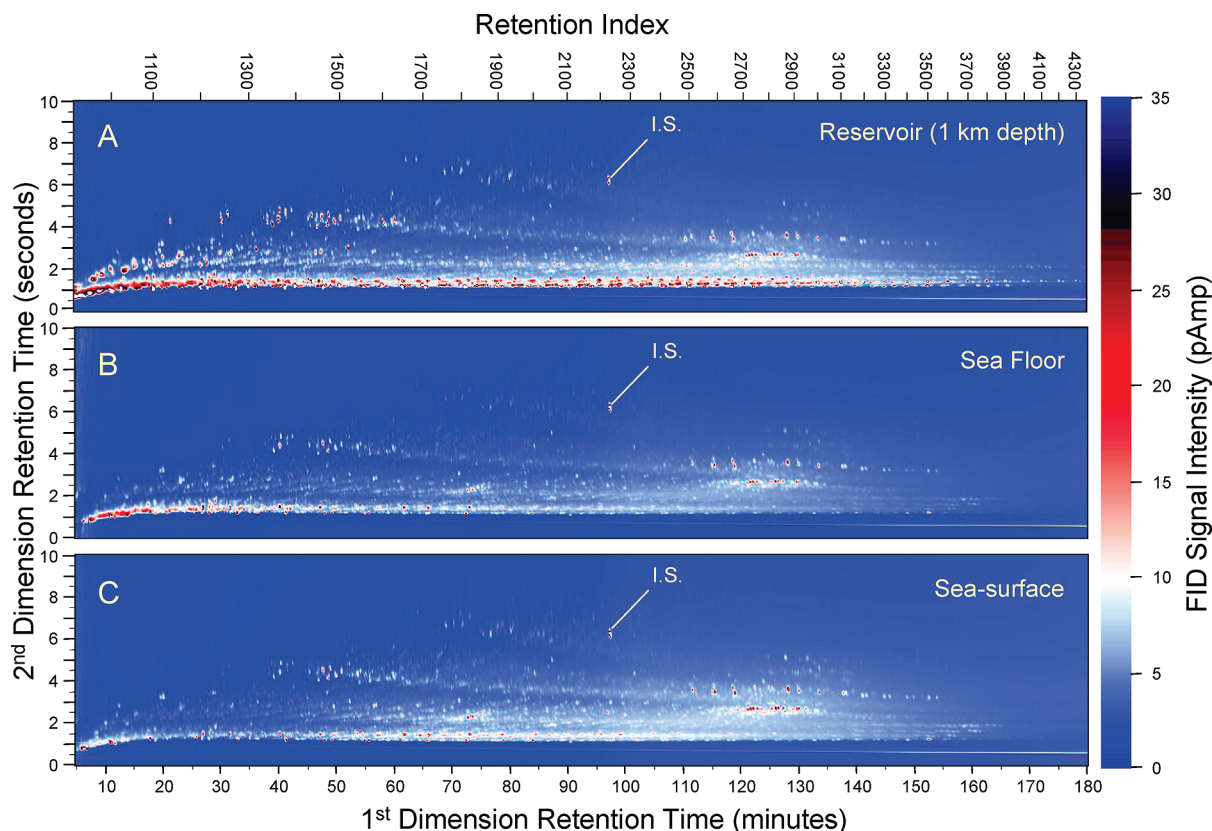


FIGURE 1. GC \times GC-FID chromatograms of (A) crude oil from Platform Holly (Well 3242–15; 34°23.370 N, 119°53.258 W), (B) oil collected as it was emerging from the sea floor at Jackpot Seep, and (C) a droplet of oil collected as it was spreading on the sea surface above Jackpot Seep. Blue corresponds to the base-plane; individual white markings correspond to small peaks (compounds at low concentrations); red corresponds to large peaks (compounds at high concentrations). Visual trends represent compound classes as are shown on annotated chromatograms in Nelson et al. (8). Each image was normalized to a suite of 27 hopane and sterane biomarker molecules as described in the Supporting Information. The annotation, I.S., denotes the elution position of the internal standard, DDTP. The retention index employed throughout this manuscript (8) is used for comparing retention between samples analyzed under varying temperature programs or between samples analyzed on different chromatographs.

coelution of analytes. Resolved compounds range in size by containing 10–43 carbons. Normal-alkanes, alkylbenzenes, alkynaphthalenes, acyclic isoprenoids, and other branched alkanes collectively represent 40% of the reservoir petroleum hydrocarbon mass. The concentrations of select compounds and general compound classes are provided in SI Table S1 and Figures SI-S4–S8.

Duplicate samples collected from the sea floor and sea surface were analyzed by GC \times GC. Each set was found to be similar based on comparisons of the chromatograms, and one sample from each set was chosen for further analysis and comparison based on both chromatogram quality and similarities in retention times for known compounds when compared to each other and to samples from Platform Holly. The sea floor and sea surface samples display similar chromatographic patterns when compared to the petroleum found in the reservoir (Figure 1), particularly for biomarker compounds (see the annotated chromatograms in SI Figure SI-S2 for compound elution patterns). The concentration and distribution of tricyclic terpanes, hopanes, steranes (see SI Table S1 and Figures SI-S4–S8) and compound classes such as the total contributions of acyclic alkanes, cycloalkanes, and alkylbenzenes (see SI Figures SI-S7 and SI-S8) are consistent with the interpretation that the three samples share a common source. This is further supported through comparison to other oils (see SI Figures SI-S3–S8) including one from a distant reservoir within the Monterey Formation (Platform Gail E-16 L) and one from a formation in Oman (Arabian light crude).

Subsurface Transformations by Anaerobic Biodegradation.

To identify the compositional changes between the

reservoir source oil and the oil emitted from the sea floor, we prepared a difference chromatogram of the sea floor sample minus the reservoir sample (Figure 2A) (8). This figure reveals that several compound groups were degraded during ascent from the reservoir to the sea floor. Losses of *n*-alkanes and other saturates as well as select aromatics including low-molecular-weight alkyl-substituted naphthalenes, and alkyl-substituted benzenes are observed. Compound classes displaying the greatest losses between the subsurface and sea floor include many of the components present at high concentration in the reservoir oil, such as *n*-alkanes, branched alkanes, acyclic isoprenoids, monocyclic alkanes, alkylbenzenes, and alkynaphthalenes (Table 1). As shown in Table 1, *n*-alkanes and *n*-alkylbenzenes, which, respectively, represent 10.9 and 8.1% of total GC-amendable TPHs in the reservoir, are quantitatively removed. Acyclic isoprenoids and branched alkanes collectively represent 17.5% of the TPHs in the reservoir and are found to decrease by 85%. The percentage losses between the subsurface and sea floor is tabulated for over 180 individual compounds in SI Table S1.

The observed losses of these compound classes are typical of biodegradation (20–22), and the differences between the seeping and reservoir petroleum hydrocarbon compositions were attributed to biodegradation in the subsurface. This interpretation was tested independently by examining the chromatograms for evidence of hydrocarbon evaporation or dissolution during this transition (Figure 3). This analysis is possible because GC \times GC uniquely enables the quantitative elucidation of hydrocarbon phase transfers to air (evaporation or gas washing) and water (dissolution). Patterns of phase transfer are distinguishable because the position of a peak

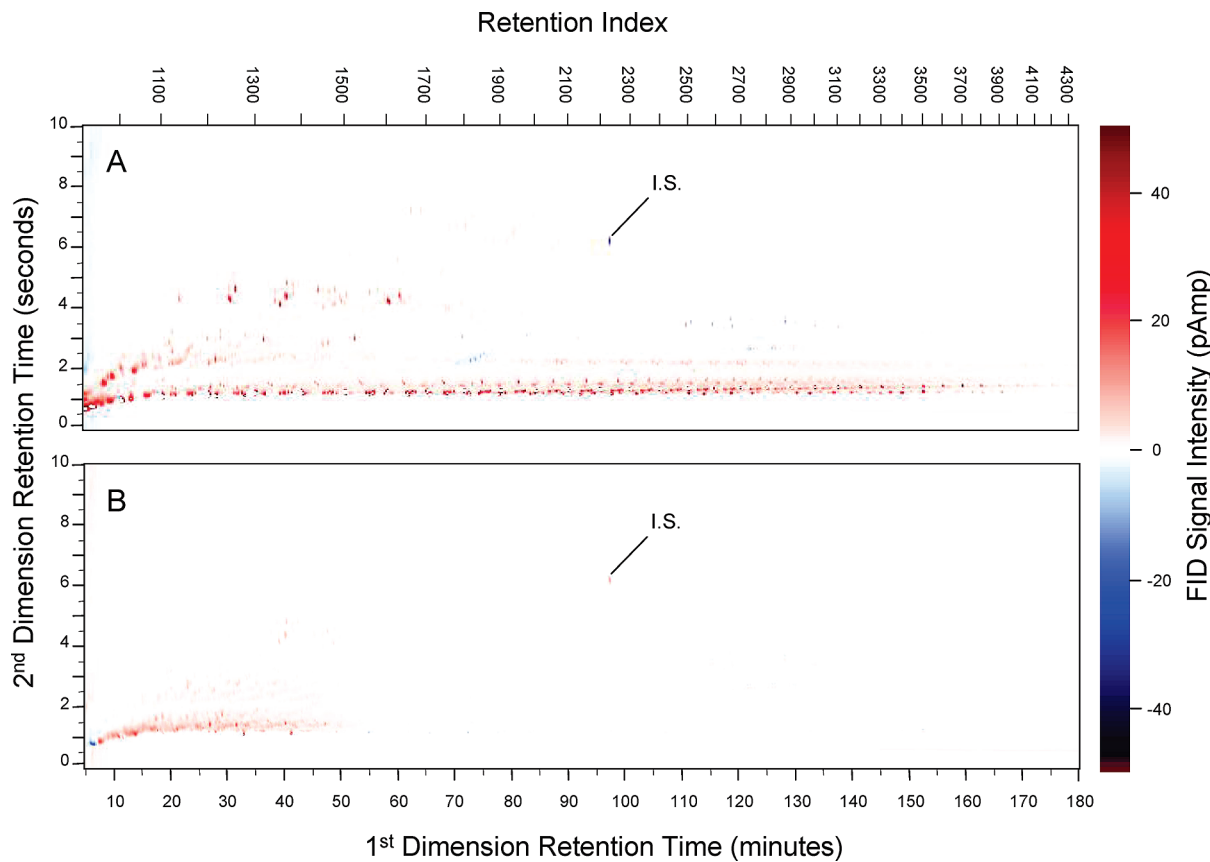


FIGURE 2. Difference chromatograms produced by (A) subtracting the chromatogram of a sea floor sample (Figure 1B) from the chromatogram of a reservoir sample (Figure 1A) and (B) by subtracting the chromatogram of a sea surface sample (Figure 1C) from the chromatogram of a sea floor sample (Figure 1B). The base-plane appears white, while compounds at a higher concentration in the reservoir sample (A; Figure 1A) and the sea floor sample (B; Figure 1B) appear red. Compounds at higher concentrations in the sea floor sample (A; Figure 1B) and the sea surface sample (B; Figure 1C) appear blue and compounds with little difference in concentration in both samples vanish. These difference chromatograms highlight both the (A) biodegradation of abundant hydrocarbons that occurs in the subsurface as well as (B) the physical processes acting to alter the hydrocarbon composition of the crude oil from the time it reaches the sea floor until its eventual transit to the sea surface. I.S., in the middle of the chromatograms denotes the elution position of the standard, DDTP.

TABLE 1. Total Petroleum Hydrocarbon Balance for Reservoir, Sea Floor, and Sea Surface Samples Collected at Coal Oil Point, CA

compound classes	reservoir ^a	sea floor ^a		sea surface ^a	
	% contribution of TPH ^b	% contribution of TPH ^b	% loss from reservoir ^c	% contribution of TPH ^b	% loss from reservoir ^d
n-alkanes	11	0	100	0	100
branched alkanes	18	5.1	85	5.4	81
n-alkylcyclopentanes	0.8	0.3	81	0.2	85
n-alkylcyclohexanes	0.8	0.3	74	0.3	78
n-alkylbenzenes	8.1	0	100	0	100
alkylnaphthalenes ^e	0.4	0.1	83	0.1	91

^a Petroleum samples collected from Platform Holly reservoir 3242–15, the sea floor, and from the sea surface.

^b Contribution of hydrocarbon class to the total petroleum hydrocarbons found in the sample. ^c The percent of hydrocarbons lost during transit from the reservoir to the sea floor. ^d The percent of hydrocarbons lost during transit from the reservoir to the sea surface. ^e Includes naphthalene, 2-methylnaphthalene, 1-methylnaphthalene, 1-ethylnaphthalene, and 2,6-dimethylnaphthalene (SI Table SI-S1).

within a two-dimensional chromatogram can be rigorously related to the volatility and aqueous solubility of the corresponding hydrocarbon compound (9). When comparing GC×GC chromatograms of different samples, we can identify signatures of evaporation and dissolution as systematic mass loss trends with respect to compound volatility and solubility (5). This is the first study in which different sample chromatograms are sufficiently aligned to allow visualization of evaporation and dissolution signatures in the completely resolved GC×GC chromatogram space. A comparison of sea

floor oil and reservoir oil samples showed no systematic evidence of significant mass losses due to evaporation or dissolution (Figure 3B). This supports our interpretation that biodegradation, rather than gas-washing or water-washing in the reservoir, caused the observed compound losses. To identify biodegradation trends among compounds less abundant than those visualized in difference chromatograms (Figure 2A and B), an algorithm was developed to track compounds between similarly sourced samples based on GC×GC retention times. The algorithm compared the

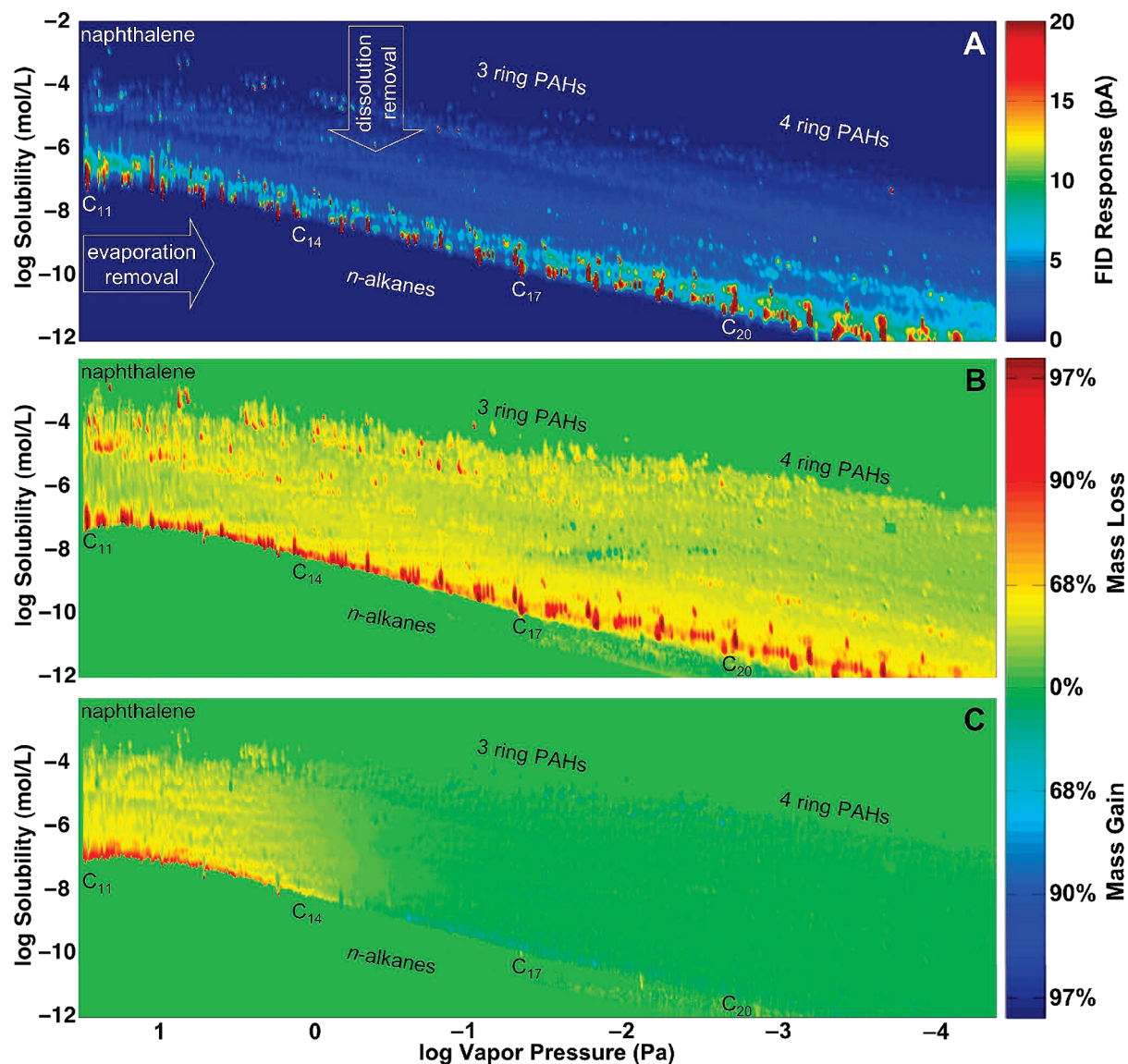


FIGURE 3. GC \times GC chromatograms elucidate signatures indicative of hydrocarbon phase transfer to air and water (5). In each panel the 1st and 2nd dimension retention times have been directly transformed into hydrocarbon volatility and aqueous solubility, respectively (9). (A) The reservoir sample chromatogram is transformed into a map of composition (detector response) plotted with respect to volatility (x-axis) and aqueous solubility (y-axis) of the analytes. Labeled arrows indicate the expected paths of mass transfer signatures; evaporation and dissolution should progressively remove mass along the axes of volatility and solubility, respectively (6). In the subsequent panels, hydrocarbon compositional changes with respect to volatility and aqueous solubility are depicted for (B) the reservoir sample to sea floor sample transition and (C) the sea floor sample to sea surface sample transition. Panels B and C were generated by evaluating the mass ratio between the two sample chromatograms (each normalized to a suite of 27 hopane and sterane molecules) and then redistributing this mass ratio information as a plot of volatility versus solubility. Observed trends of mass loss and mass gain suggest that (B) the sea floor sample is heavily biodegraded with respect to the reservoir sample rather than evaporated or dissolved. There is no clear evidence for phase transfer in the subsurface; supporting the interpretation that biodegradation is the responsible mass loss process. By contrast, (C) the sea surface sample is partly evaporated relative to the sea floor sample, showing an estimated 10% TPHs loss.

chemical compositions of reservoir, seep, and samples collected from the sea surface overlying the seep (see SI section SI-3 for algorithm details). This comparison resulted in a successful tracking of \approx 1400 compounds, which was equivalent to approximately one-quarter of the total number of different hydrocarbons resolved in the GC \times GC chromatograms. We estimate that \approx 72% (981 peaks) of tracked compounds exhibited a significant decrease in concentration (i.e., a concentration decrease exceeding our estimated peak volume error of \pm 34% at the 95% confidence interval), whereas only \approx 2.9% (39 peaks) of the compounds showed a significant concentration increase (Figure 4). There is no obvious preference for saturated or aromatic hydrocarbon loss, nor is there a bias based on the initial concentration

(Figure 4), molecular weight, volatility, or solubility (Figure 3B). Importantly, this algorithm excludes compounds that are degraded completely, such as most n-alkanes and many of the other compounds given in SI Table S1. Based on the sheer number and diversity of degraded compounds, it appears that there is a level of generality in the metabolic preference of anaerobic, hydrocarbon-degrading communities that was not previously known to exist (3) which substantially changed the molecular composition of the reservoir oil prior to reaching the sea floor.

The subsurface environment underlying the COP seeps are likely anoxic. Gases and production water collected from the reservoirs underlying the seeps contain abundant reduced chemicals such as hydrogen sulfide and ferrous iron (13),

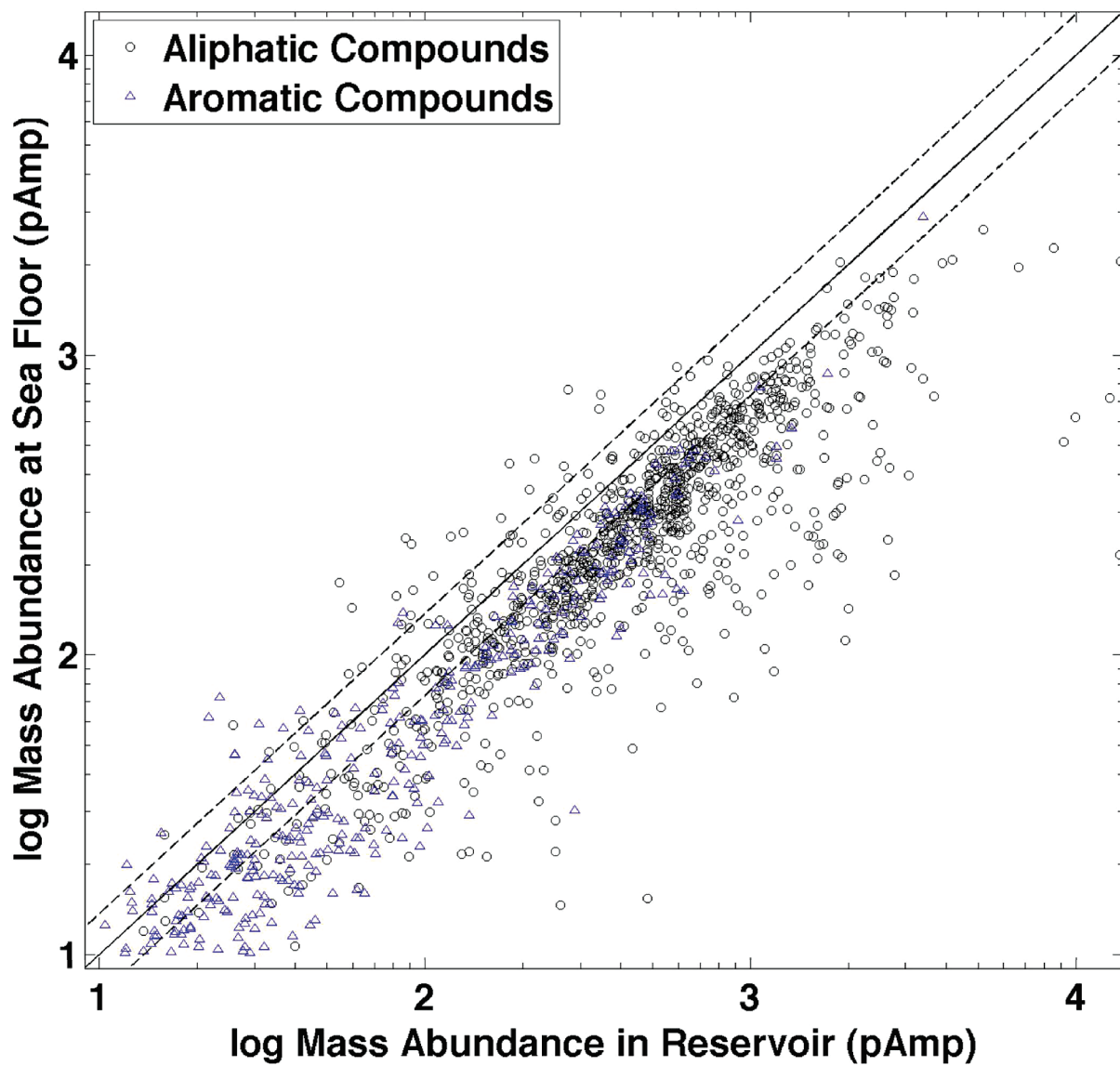


FIGURE 4. A comparison of mass abundances of 1363 individually tracked compounds in the reservoir oil and sea floor seep oil. Both samples were normalized to the aggregated mass of a suite of 27 hopane and sterane biomarker compounds. We estimated an analytical uncertainty of $\pm 34\%$ (for the 95% confidence interval) in the mass abundance of each compound, but individual error bars are not included as they diminish visual clarity. Consequently, the mass abundance uncertainty is instead depicted as a 34% error in the 1:1 line (dashed lines). Points falling below the lower dashed line indicate a significant mass loss in the sea floor seep relative to the reservoir oil. Points above the upper dotted line indicate a significant mass gain. Completely degraded compounds in SI Table S1–S1 are excluded by the peak finding algorithm.

and production waters drawn from the reservoir are known to harbor populations of strictly anaerobic prokaryotes including methanogens (14, 17). Sediments overlying seeps within the COP field maintain high rates of sulfate reduction (23). Seep gas has the odor of hydrogen sulfide, is devoid of oxygen, and supports active populations of sulfide-oxidizing bacteria (23). As such, anaerobic metabolic processes linked to petroleum consumption are likely to characterize the activity of the subsurface microbial community in this environment. The penetration of seawater into the reservoir may provide sufficient sulfate to support dissimilatory sulfate reduction locally. However, the presence of methanogens in reservoir waters (14) and the presence of mixed thermogenic-biogenic methane in some seeps implicates methanogenesis as an important pathway driving petroleum degradation (23, 24).

These results provide important insights on the activity of petroleum-degrading microbes in the subsurface. The metabolic activity of oil-degrading communities from subsurface reservoirs is typically thought to bypass most

heteroatomic compounds containing N, O, or S atoms and cause a progressive loss of light hydrocarbons (21). Petroleum biodegradation rates are not well constrained but anaerobic oxidation rates are believed to be orders of magnitude slower than aerobic hydrocarbon biodegradation rates (21). Normal-alkanes and isoalkanes are removed first during microbial petroleum degradation followed by branched and cycloalkanes and then progressing through alkyl and multiring cycloalkanes with multiring compounds containing three or more aromatic rings being the most resistant (21). Results shown here indicate that biodegradation preference likely acts on a continuum of compounds. That is, hundreds to thousands of compounds appear to be simultaneously metabolized by the microbial community at varying rates, resulting in the distribution of losses shown in Figures 2A and 4. These results support those reported by Larter et al. (25, 26), and Prince and Suflita (27), but our observations dramatically increase and the number hydrocarbons known to be biodegraded. Several unanticipated trends were also observed in the results, including increased recalcitrance of

long chain ($\sim\text{C}_{38}\text{--C}_{42}$) isoprenoids with increasing cyclization (SI Table S1), equivalent biodegradation of 1- and 2-methylnaphthalenes, and the preferential or simultaneous loss of long chain alkylcyclopentanes and alkylcyclohexanes over short chain analogs (see SI Figure SI-S9); the latter observation seemingly supports those made by Siddique et al. (2006) and Hostettler et al. (2007) (28, 29). While these samples represent only snap-shots of hydrocarbon biodegradation, the number and diversity of degraded compounds supports a perspective of broad metabolic specificity. These results further demonstrate a capacity for anaerobic microbial communities to consume diverse hydrocarbons beyond those typically investigated, with implications for discovery of novel metabolic actions. The complete or partial biodegradation for over one thousand hydrocarbons, as shown here, stands in stark contrast to only a handful of known pathways for hydrocarbon biodegradation by strictly anaerobic microbes (3).

Volatilization Drives Initial Compositional Changes of Seeping Oil. Analysis of sample chromatograms showed that select hydrocarbon components evaporated very rapidly when the oil bubbled from seeps and reached the sea surface. To interrogate whether evaporation or dissolution acted broadly on the oil emitted from the sea floor seep, we evaluated mass loss trends with respect to hydrocarbon volatility and solubility for the sea surface sample compared to the sea floor sample (Figure 2B and 3C). Duplicate samples at the sea surface show significant mass loss with respect to hydrocarbon volatility when compared to sea floor samples (mass loss trends are shown for only one of the two sea surface samples; Figure 3C). Based on duplicate samples of droplets escaping from the sea floor and captured during midascent through the water column (not shown), the ascending oil did not change significantly during traversal of the water column. At the sea surface, an estimated 10% TPBs mass loss occurred within seconds or minutes, giving rise to the strong evaporation signature observed in the sea surface samples.

The observed phase transfer rates of $\sim\text{C}_{12}\text{--C}_{15}$ hydrocarbons at the sea surface are rapid compared to expected rates based on gas–liquid boundary layer considerations. The ≈ 1 cm diameter oil droplets that were sampled had traversed the water column within minutes, and they displayed spontaneous surface-tension-driven spreading upon arrival at the sea surface. We employed a simple boundary-layer-based mass transfer calculation that had previously been applied to evaporation and dissolution rates of oil components (10). These estimates suggest that for a resting oil blob of ≈ 3 mm thickness, the observed mass losses would require about a week of exposure at the surface. However, the blobs were collected within 10–20 seconds of their arrival at the sea surface. Two interpretations are suggested to explain this apparent contradiction. One explanation for this phenomenon is that spontaneous spreading at an air–water interface may fractionate volatile compounds based on differences in surface tension among hydrocarbon constituents, and the resulting compositional changes resemble an evaporative signature. Alternatively, the oil droplet may have mixed with the thin slick of oil that had been resting at the surface for a longer period of time. According to our mass transfer calculations, such a resting slick (assumed 3×10^{-4} mm thick (30)) would exhibit significant evaporative losses of $\text{C}_{12}\text{--C}_{15}$ -range hydrocarbons within minutes. Hence, a mixture of the two materials (newly arrived sea surface droplet and resting oil slick) may explain the observed evaporation signature in collected samples.

Using GC \times GC to Investigate Petroleum Weathering in Natural Marine Seeps. This work provides an extensive description of the compounds found in seeping oil and is the first to differentiate molecular transformations arising

from the processes of dissolution, evaporation and biodegradation in the seep environment. Biodegradation is viewed here as a natural attenuator of petroleum hydrocarbon flux and economic value, and acts to decrease seepage in this region through the removal of numerous and diverse hydrocarbons. Anaerobic biodegradation in the subsurface induces mass loss signatures that are dramatically different from the observed evaporation signature at the sea surface. These results provide a new basis for understanding the molecular transformations of petroleum as it migrates from the deep subsurface and becomes influenced by the biosphere, hydrosphere, and atmosphere. These processes are especially important given that natural seeps constitute approximately half of all oil inputs to the sea (31).

Acknowledgments

We thank S. Horner and Venoco Inc. for providing access to reservoir samples. We also thank J. Boles for providing advice on the geologic structure of the COP field. We acknowledge support from the U.S. National Science Foundation (OCE-0447395 to D.L.V. and IIS-0430835 to C.M.R.), the U.S. Minerals Management Service (Task 85338 to D.L.V.), the California Toxic Substance Research and Training Program (19909 to G.D.W.), the U.S. Department of Energy (DE-FG02-06ER15775 to C.M.R.) and to the Seaver Institute for support and assistance with the GC \times GC system.

Supporting Information Available

A detailed description of the analytical methods employed in this study along with an extensive list of monitored compounds with their respective concentrations and figures supporting the interpretation and conclusions reported here. This material is available free of charge via the Internet at <http://pubs.acs.org>.

Literature Cited

- Hunt, J. S. *Petroleum Geochemistry and Geology*; W. H. Freeman: New York, 1996.
- Wang, Z.; Fingas, M. F. Development of oil hydrocarbon fingerprinting and identification techniques. *Mar. Pollut. Bull.* **2003**, *47*, 423–452.
- Spormann, A. M.; Widdel, F. Metabolism of alkylbenzenes, alkanes, and other hydrocarbons in anaerobic bacteria. *Bio-degradation* **2000**, *11* (2–3), 85–105.
- Van Hamme, J. D.; Singh, A.; Ward, O. P. Recent advances in petroleum microbiology. *Microbiol. Mol. Biol. Rev.* **2003**, *67* (4), 503–549.
- Arey, J. S.; Nelson, R. K.; Reddy, C. M. Disentangling oil weathering using GC \times GC. 1. Chromatogram analysis. *Environ. Sci. Technol.* **2007**, *41* (16), 5738–5746.
- Reddy, C. M.; Eglington, T. I.; Hounshell, A.; White, H. K.; Xu, L.; Gaines, R. B.; Frysinger, G. S. The West Falmouth oil spill after thirty years: The persistence of petroleum hydrocarbons in marsh sediments. *Environ. Sci. Technol.* **2002**, *36* (22), 4754–4760.
- Frysinger, G. S.; Gaines, R. B.; Xu, L.; Reddy, C. M. Resolving the unresolved complex mixture in petroleum-contaminated sediments. *Environ. Sci. Technol.* **2003**, *37* (8), 1653–1662.
- Nelson, R. K.; Kile, B. S.; Plata, D. L.; Sylva, S. P.; Xu, L.; Reddy, C. M.; Gaines, R. B.; Frysinger, G. S.; Reichenbach, S. E. Tracking the weathering of an oil spill with comprehensive two-dimensional gas chromatography. *Environ. Forensics* **2006**, *7* (1), 33–44.
- Arey, J. S.; Nelson, R. K.; Xu, L.; Reddy, C. M. Using comprehensive two-dimensional gas chromatography retention indices to estimate environmental partitioning properties for a complete set of diesel fuel hydrocarbons. *Anal. Chem.* **2005**, *77* (22), 7172–7182.
- Arey, J. S.; Nelson, R. K.; Plata, D. L.; Reddy, C. M. Disentangling oil weathering using GC \times GC. 2. Mass transfer calculations. *Environ. Sci. Technol.* **2007**, *41* (16), 5747–5755.
- Hornafius, J. S.; Quigley, D.; Luyendyk, B. P. The world's most spectacular marine hydrocarbon seeps (Coal Oil Point, Santa Barbara Channel, California): quantification of emissions. *J. Geophys. Res., [Oceans]* **1999**, *104* (C9), 20703–20711.

- (12) Kvenvolden, K. A.; Cooper, C. K. Natural seepage of crude oil into the marine environment. *Geo-Mar. Lett.* **2003**, *23* (3–4), 140–146.
- (13) Reed, W. E.; Kaplan, I. R. The chemistry of marine petroleum seeps. *J. Geochem. Explor.* **1977**, *7* (2), 255–293.
- (14) Orphan, V. J.; Taylor, L. T.; Hafenbradl, D.; DeLong, E. F. Culture-dependent and culture-independent characterization of microbial assemblages associated with high-temperature petroleum reservoirs. *Appl. Environ. Microbiol.* **2000**, *66* (2), 700–711.
- (15) Boles, J. R.; Eichhubl, P.; Garven, G.; Chen, J. Evolution of hydrocarbon migration pathway along a basin bounding fault: evidence from fault cements. *AAPG Bull.* **2004**, *88* (7), 947–970.
- (16) Hill, T. M.; Kennett, J. P.; Valentine, D. L.; Yang, Z.; Reddy, C. M.; Nelson, R. K.; Behl, R. J.; Robert, C.; Beaufort, L. Climatically driven emissions of hydrocarbons from marine sediments during deglaciation. *Proc. Nat. Acad. Sci. U. S. A.* **2006**, *103* (37), 13570–13574.
- (17) Orphan, V. J.; Boles, J. R.; Goffredi, S. K.; DeLong, E. F. Geochemical influence on diversity and microbial processes in high temperature oil reservoirs. *Geomicrobiol. J.* **2003**, *20* (4), 295–311.
- (18) Gaines, R. B.; Frysinger, G. S.; Reddy, C. M.; Nelson, R. K. Oil spill source identification by comprehensive two-dimensional gas chromatography (GC \times GC) In *Oil Spill Fingerprinting and Source Identification*, Chapter 5; Wang, Z., Stout, S. Eds.; Elsevier Science: New York, 2006.
- (19) Quigley, D. C.; Hornafius, J. S.; Luyendyk, B. P.; Francis, R. D.; Clark, J.; Washburn, L. Decrease in natural marine hydrocarbon seepage near Coal Oil Point, California, associated with offshore oil production. *Geology* **1999**, *27* (11), 1047–1050.
- (20) Peters, K. K.; Walters, C. C.; Moldowan, J. M. *The Biomarker Guide, Biomarkers and Isotopes in Petroleum Exploration and Earth History*; 2nd ed.; Cambridge University Press: Cambridge, MA, 2005; Vol. 1.
- (21) Peters, K. K.; Walters, C. C.; Moldowan, J. M. *The Biomarker Guide, Biomarkers and Isotopes in the Environment and Human History*; 2nd ed.; Cambridge University Press: Cambridge, MA, 2005; Vol. 2.
- (22) Wenger, L. M.; Davis, C. L.; Isaksen, G. H. *Multiple Controls on Petroleum Biodegradation and Impact in Oil Quality*, Paper 71450; Society of Petroleum Engineers: Houston, TX, 2001.
- (23) Bauer, J. E.; Montagna, P. A.; Spies, R. B.; Hardin, D. D.; Prieto, M. Microbial biogeochemistry and heterotrophy in sediments of a marine hydrocarbon seep. *Limnol. Oceanogr.* **1988**, *33* (6), 1493–1513.
- (24) Jones, D. M.; Head, I. M.; Gray, N. D.; Adams, J. J.; Rowan, A. K.; Aitken, C. M.; Bennett, B.; Huang, H.; Brown, A.; Bowler, B. F. J.; Oldenburg, T.; Erdmann, M.; Larter, S. R. Crude oil biodegradation via methanogenesis in subsurface petroleum reservoirs. *Nature* **2008**, *451* (7175), 176–180.
- (25) Larter, S. R.; Wilhelms, A.; Head, I. M.; Koopmans, M.; Aplin, A.; Di Primio, R.; Zwach, C.; Erdmann, M.; Telnaes, N. The controls on the composition of biodegraded oils in the deep subsurface: Part I—Biodegradation rates in petroleum reservoirs. *Org. Geochem.* **2003**, *34* (4), 601–613.
- (26) Larter, S. R.; Huang, H.; Adams, J.; Bennett, B.; Jokanola, F.; Oldenburgh, T.; Jones, M.; Head, I. M.; Riediger, C.; Fowler, M. The controls on the composition of biodegraded oils in the deep subsurface: Part II — Geological controls on subsurface biodegradation fluxes and constraints on reservoir-fluid property prediction. *AAPG Bull.* **2006**, *90* (6), 921–938.
- (27) Prince, R. C.; Sulfita, J. M. Anaerobic biodegradation of natural gas condensate can be stimulated by the addition of gasoline. *Biodegradation* **2007**, *18* (4), 515–523.
- (28) Siddique, T.; Fedorak, P. M.; Foght, J. M. Biodegradation of short-chain n-alkanes in oil sands tailings under methanogenic conditions. *Environ. Sci. Technol.* **2006**, *40* (17), 5459–5464.
- (29) Hostettler, F. D.; Wang, Y.; Huang, Y.; Cao, W.; Bekins, B. A.; Rostad, C. E.; Kulpa, C. F.; Laursen, A. Forensic fingerprinting of oil-spill hydrocarbons in a methanogenic environment-Mandan, ND and Bemidji, MN. *Environ. Forensics* **2007**, *8* (1–2), 139–153.
- (30) Allen, A.; Schlueter, R.; Mikolaj, P. Natural oil seepage at Coal Oil Point, Santa Barbara, California. *Science* **1970**, *170* (3934), 974–977.
- (31) National Research Council *Oil in the Sea III: Inputs, Fates, and Effects*; National Academies Press: Washington, DC, 2003.

ES8013908